Transactions on Energy Systems and Engineering Applications

Article

Surface wettability analysis using a microdroplet: a numerical approach

Ganesh Sahadeo Meshram[1,*], Gloria Biswal[1] and Ashish B Khelkar[2]

[1] Department of Mechanical Engineering, IIT Kharagpur, Kharagpur, 721302 India.
[2] Department of Mechanical Engineering, NIT Meghalaya, Shillong, 793003 India.
[*] Correspondence: ganeshmeshram.iitkgp@gmail.com

Received: 25 April 2024; Accepted: 15 November 2024; Published: 10 March 2025

Abstract: Analysis of hydrophobicity is essential for learning about the characteristics of molecules, surfaces, and materials that reject water. Using a two-dimensional (2D) pseudo-potential multiphase lattice Boltzmann approach with a $D2Q9$ model, this work examines the influence of solid-fluid interaction strength on wettability and hydrophobicity of smooth surfaces. To ascertain the contact angle and assess the accuracy of the numerical model, the study considers the equilibrium state of a water droplet on a smooth surface. In a $200x200$ lattice unit domain, droplets having a radius of 60 lattice units are used to assess the hydrophobicity of smooth surfaces. According to the research, there is a large rise in the contact area between solid walls and water droplets when the solid-fluid interaction parameter is raised, which leads to a greater degree of hydrophobicity. By measuring the contact angle between the solid and fluid-vapor interface for different surfaces, it is observed that as G_{ads} becomes more negative, the contact angle decreases, indicating increased surface hydrophobicity and effect of on droplet spreading also highlighted in the research.

1. Introduction

Surface wettability, which refers to an ability of the liquid to spread or bead on a solid surface, is crucial for a variety of industrial and scientific uses, such as the creation of microfluidic devices and materials [1, 2]. To optimize surfaces for liquid manipulation, adhesion, and friction, it is essential to understand and quantify this phenomenon at the microscale [3]. Recently, the detailed knowledge of the complex interactions between liquids and solid substrates made possible by numerical approaches has revolutionized surface wettability research [4–6]. Using a microdroplet as a probing tool, this work uses advanced numerical simulations to evaluate surface wettability to better understand the complicated dynamics at the interface. Researchers may now analyze phenomena at previously unreachable scales thanks to the innovative and accurate approach brought about by the use of microdroplets in surface wettability research.

How to cite this article: Meshram, Ganesh; Biswal, Gloria; Khelkar, Ashish. Surface wettability analysis using a microdroplet: a numerical approach. *Transactions on Energy Systems and Engineering Applications*, 6(1): 676, 2025. DOI:10.32397/tesea.vol6.n1.676

This study uses computational techniques to replicate the behavior of liquid molecules at the interface, delving into the minute details of a droplet interaction with a solid surface [7]. By using this numerical framework, we want to close the knowledge gap between theory and practice by providing a solid platform for investigating and modifying surface wettability. Recent work has focused a great deal of emphasis on investigating surface wettability utilizing a microdroplet and a numerical technique, demonstrating an increasing interest in comprehending and controlling interfacial processes at the microscale. Johnson et al. [8, 9] made a groundbreaking addition to this field of study by developing a computational framework based on molecular dynamics modeling to study the behavior of microdroplets on different surfaces. Their study showed how numerical approaches may capture complex wetting dynamics and also showed how surface qualities can be optimized by adjusting factors like chemical composition and surface roughness. Building on this, Adam et al. [4, 5] expanded the numerical method to include dynamic wetting situations, enabling a more thorough investigation of the evolution of microdroplets over time on various surfaces. This development was documented by sophisticated numerical simulations, which unveiled fresh perspectives on the intricate interactions between liquid and solid at the microscale and served as a vital first step for further investigations.

The use of lattice Boltzmann techniques to examine microdroplet dynamics on surfaces has also revolutionized the field of research. Chen et al. [8] conducted groundbreaking research to examine how surface topography affects microdroplet behavior using lattice Boltzmann simulations. Their study demonstrated the flexibility of the lattice Boltzmann approach in capturing complex wetting patterns by numerically simulating the fluid dynamics at the mesoscale, highlighting the significance of taking surface texture into account in understanding overall wettability. This work was a major breakthrough by proving that numerical methods, in particular lattice Boltzmann simulations, are effective in fully addressing the intricate details of microdroplet behavior on textured surfaces. The work of Muto et al. [10, 11] has broadened the scope of numerical experiments by taking into account how temperature and pressure affect microdroplet wetting as the subject continues to develop. Their study used a multiscale numerical technique to clarify the thermodynamic factors controlling microdroplet behavior by integrating lattice Boltzmann methods with molecular dynamics simulations. The multidisciplinary character of surface wettability analysis is shown by this integration of many numerical approaches, highlighting the need for a comprehensive understanding that takes into account both macroscopic thermodynamic effects and microscale dynamics. The combined knowledge from these investigations emphasizes how important numerical methods are to improving our understanding of surface wettability with microdroplets and provides a flexible toolbox for scientists and industry practitioners working in a variety of fields. The present work lies in its systematic analysis of the relationship between solid-fluid interaction strength and surface hydrophobicity using the 2D pseudo-potential multiphase Lattice Boltzmann method, which has not been explored in previous literature. Additionally, the effects on velocity streamlines and droplet spreading are comprehensively analyzed.

2. Numerical Methodology

The lattice-Boltzmann equation is used to estimate the distribution function f_k at each time step and node. The link between the Navier-Stokes and continuity equations is explained using the Chapman-Enskog perturbation expansion method [10, 12]. The equation for distribution function is determined in the following manner using the lattice-Boltzmann method:

$$f_p(x + e_p\delta t, t + \delta t) - f_p(x, t) = \Omega_p(x, t), \tag{1}$$

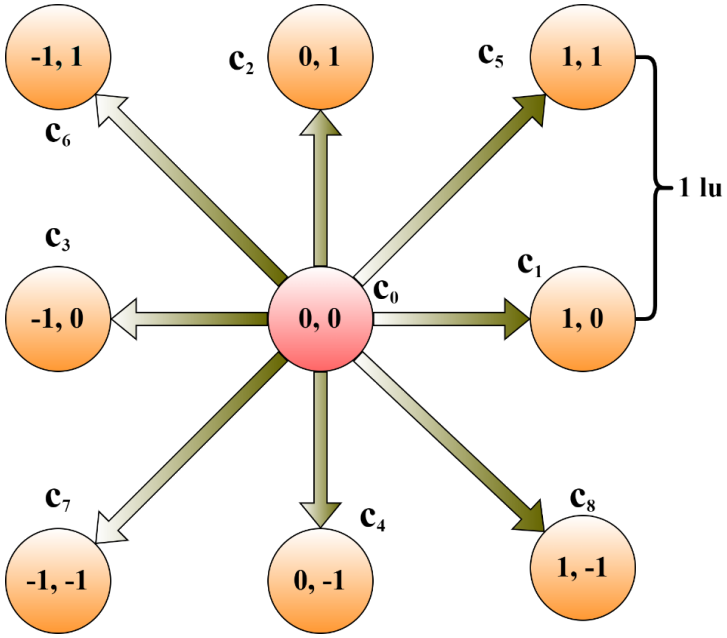

Figure 1. *D*2*Q*9 model with directions and their discrete velocities used in this simulation.

$$f_p^{eq}(x,t) = \rho\omega_p \left[1 + \frac{e_p \cdot u}{c_{ls}^2} + \frac{(e_p \cdot u)^2}{2c_{ls}^2} - \frac{u^2}{2c_{ls}^2}\right], \tag{2}$$

where, f_p is the density distribution function, f_p^{eq} is the equilibrium density function, x is the spatial coordinate, e_p is the particle velocity along the direction p, ω_p is the weighting coefficient, $c_{ls} = c/\sqrt{3}$ is the sound speed of a lattice, and $c = \delta x/\delta t$ denotes lattice speed, δx denotes lattice space step, and u is macroscopic velocity.

The *D*2*Q*9 model is most suitable for two-dimensional problems and its representation is as shown in Figure 1. Weighting coefficients are defined as follows:

$$\begin{aligned} w_p &= \begin{cases} 4/9, & p = 0 \\ 1/9, & p = 1,2,3,4 \\ 1/36, & p = 5,6,7,8 \end{cases} \\ e_p &= \begin{cases} (0,0), & p = 0 \\ (\pm 1,0)c, (0,\pm 1)c, & p = 1,2,3,4 \\ (\pm 1,\pm 1)c, & p = 5,6,7,8 \end{cases} \end{aligned}. \tag{3}$$

The lattice Boltzmann equation can be solved in two steps: collision and streaming.

Collision

When particles arriving at a node collide and change their direction, the distribution function after the collision is calculated as

$$f_p^{out}(x,t) = f_p(x + e_p\delta t) = f_p^{in}(x,t) - \frac{1}{\tau}\left[f_p^{in}(x,t) - f_p^{eq}(x,t)\right]. \tag{4}$$

Streaming

The particles move to adjacent nodes according to their velocity direction.

$$f_p^{in}(x + e_i\delta t, t + \delta t) = f_p^{out}(x, t + \delta t). \tag{5}$$

Also, the kinematic viscosity can be calculated using relaxation time.

$$\nu = \frac{c_{ls}^2 \delta t}{2}(2\tau - 1). \tag{6}$$

2.1. Calculation of forces

The Shan and Chen Pseudo-potential multiphase lattice Boltzmann model was conceptualized to simulate the non-local interaction among particles, as referred in [12], [9]. In the context of single-component multiphase flow, the exerted interaction force upon particles situated at a specific position **x** is manifested as follows:

$$F_{int}(x, t) = -G\psi(x, t)\Sigma_p \omega_p \psi(x + e_p\delta t, t)e_p. \tag{7}$$

Here, the G parameter is used to manipulate the strength of the interaction force. Equation for the Pseudo-potential term $\psi(x)$ is defined as

$$\psi = \sqrt{\frac{2(P - \rho c_{ls}^2)}{G c_{ls}^2}}, \tag{8}$$

where P is denoted as fluid pressure.
The solid-fluid interaction force is [13]

$$F_{ads} = \left[-G_{ads}\psi(x, t)\Sigma_p \omega_p s(x + e_p\delta t)e_p\right], \tag{9}$$

where, G_{ads} is the solid-fluid interaction parameter, $s(x + e_p\delta t)$ is the indicator function which can be written as

$$s\left(x + e_p\delta t\right) = \begin{cases} 0 & \text{if } \left(x + e_p\delta t\right) \text{ is fluid node} \\ 1 & \text{if } \left(x + e_p\delta t\right) \text{ is solid node} \end{cases}. \tag{10}$$

Total force acting at each particle x

$$F = F_{int} + F_{ads}. \tag{11}$$

The effect of gravity was neglected as the domain is in microscale where gravitational forces are negligible compared to intermolecular and surface forces.

2.2. Calculation of pressure (P)

A popular thermodynamic model for explaining the behavior of actual fluids, especially those employed in the chemical and petroleum industries, is the Peng-Robinson Equation of State (EOS). An exact expression for the pressure as a function of temperature, molar volume, and fluid composition is given by

this equation of state. The Peng-Robinson equation of state, which may represent phase equilibria under a variety of circumstances, is an advancement over the more straightforward Van der Waals equation of state.

$$P = \frac{\rho RT}{1 - b\rho} - \frac{a\rho^2 \epsilon(T)}{1 + 2b\rho - b^2\rho^2}, \tag{12}$$

$$\epsilon(T) = \left[1 + \epsilon_0 \left(1 - \sqrt{\frac{T}{T_c}}\right)\right]^2, \tag{13}$$

$$\epsilon_0 = \left(0.37464 + 1.54226\omega - 0.26992\omega^2\right).$$

Here, $R = 1, a = 2/49, b = 2/21$ and these values are adapted from the related literature on similar study [14]

2.3. Calculation of fluid density and velocity

The macroscopic density and velocity can be calculated with the help of the distribution function as

$$\Delta f_p(x,t) = f_p^{eq}(\rho(x,t), u + \Delta u) - f_p^{eq}(\rho(x,t), u), \tag{14}$$

$$\rho = \sum_k f_p = \sum_k f_p^{eq}, \tag{15}$$

$$u = \frac{1}{\rho} \sum_p f_p \cdot e_p = \sum_p f_p^{eq} \cdot e_p. \tag{16}$$

The change in velocity due to total force is written as

$$\Delta u = \frac{F\delta t}{\rho}, \tag{17}$$

and the actual fluid velocity is as follows:

$$U = u + \frac{F\delta t}{2\rho}. \tag{18}$$

At a location x and time t, the discrete particle velocity e_p is represented by the distribution function of the particle in the p^{th} direction, denoted by f_p. The lattice-Boltzmann approach explicitly solves the distribution function in two main steps at each time step. The collision operator proposed by Bhatnagar et al. [10] controls the collision step on the right side of Eq. (1), and the left side of the equation is called streaming.

$$\Omega_p(x,t) = (f_p(x,t) - f_p^{eq}(x,t))/\tau \tag{19}$$

The density distribution function can be expressed in the following way along the p^{th} direction using the Bhatnagar-Gross-Krook (BGK) collision operator:

$$f_p(x + c_p\delta t, t + \delta t) = f_p(x,t) + \delta t/\tau [f_p(x,t) - f_p^{eq}(x,t)]. \tag{20}$$

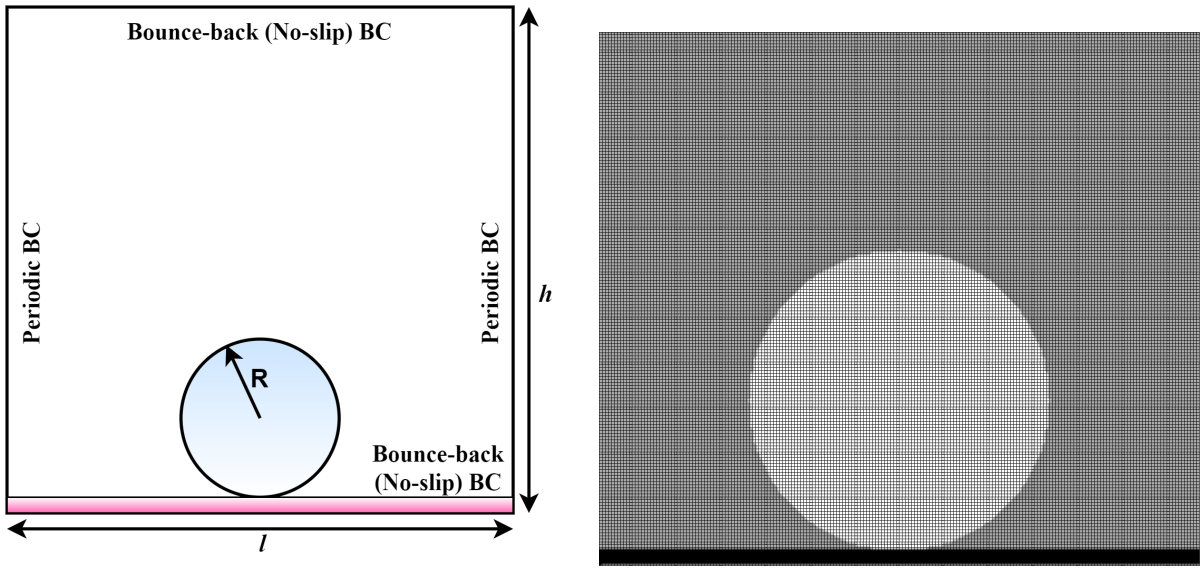

Figure 2. Problem definition along with boundary conditions (left) and mesh distribution (right).

The distribution function $f_p^{eq}(x,t)$ relies on discrete velocity and is represented by the Maxwellian equilibrium distribution function and can be written as follows:

$$f_p^{eq}(x,t) = \rho(x) w_p \left[1 + (e_p.u)/(c_{ls}^2) + ((e_p.u)^2)/(2c_{ls}^2) - u^2/(2c_{ls}^2)\right]. \tag{21}$$

2.4. Problem definition and boundary conditions

The investigation is carried out in a computational domain that is $200\mu m$ in length and $200\mu m$ in height as shown in Fig. 2 (left). The mesh distribution of the domain is uniform and structured as depicted in Fig. 2 (right). At the center of the bottom wall, a water droplet is placed with a radius of $60\mu m$ lattice units. In Fig. 2, the top, and bottom are treated as bounce-back boundary conditions, while the left and right sides of the domain are considered periodic. The use of a 2D pseudo-potential multiphase Lattice Boltzmann model for simulating static water droplets on a smooth surface with varied solid-fluid interaction parameters (G_{ads}) is evaluated in order to guarantee its correctness and consistency. Water droplet form and contact angle are examined in relation to the parameter G_{ads}. Subsequently, a comprehensive comparison and analysis were conducted, referencing a related study [14] as shown in Fig. 3. This comparison specifically delves into the static contact angle findings for solid-fluid interaction parameters ranging from -2.00 to -1.25. The simulation outcomes align remarkably well with the comparative analysis, exhibiting an error margin of no greater than 1.48%.

3. Results and discussion

3.1. Analysis of droplet spreading

Figure 4 shows the effect of the solid-fluid interaction parameter on the wettability of the smooth surfaces. The comparison is shown using the contact angle and base diameter of the water droplet for various solid-fluid interaction parameters. From Fig. 4, it is observed that the contact angle increases and the base diameter of the droplet decreases as we increase the parameter G_{ads}. This phenomenon occurs due to dominant cohesive forces between the water droplets and small adhesive forces between the water droplet and the solid wall. Figure 4 the relationship between the contact angle θ (in degrees) and base

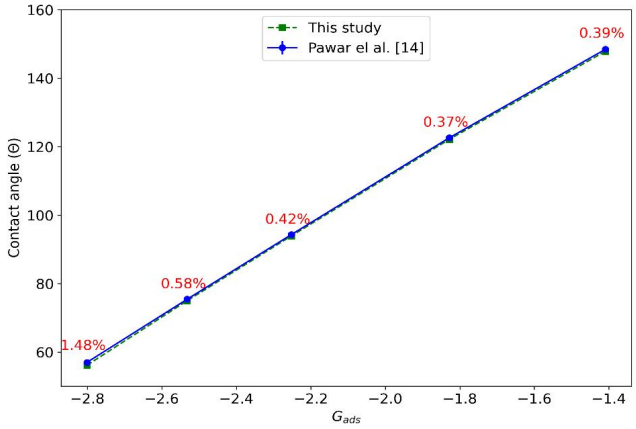

Figure 3. Validation of the model.

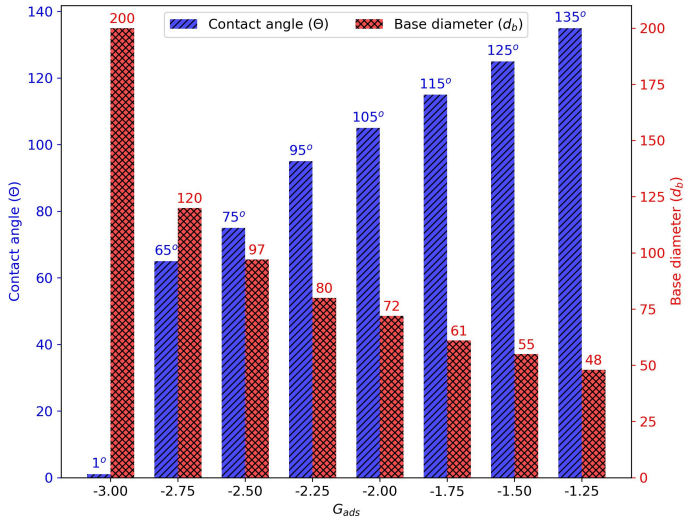

Figure 4. Contact angle and base diameter of the water droplet.

diameter d_b (in lattice units) as a function of the solid-fluid interaction parameter G_{ads}. The left vertical axis corresponds to the contact angle values, while the right vertical axis represents the base diameter. As G_{ads} increases from -3.00 to -1.25, there is a clear trend in which the contact angle increases, indicating stronger hydrophobicity. For instance, at $G_{ads} = -3.00$, the contact angle is nearly 1° and the base diameter is 200 LU, signifying maximum spreading. As G_{ads} rises to -1.25, the contact angle reaches 135°, while the base diameter reduces significantly to 48 LU, reflecting reduced spreading. Notably, the contact angle increases steadily from 65° at $G_{ads} = -2.75$ to 135° at $G_{ads} = -1.25$, while the base diameter decreases in reverse proportion, from 120 LU at $G_{ads} = -2.75$ to 48 LU at $G_{ads} = -1.25$. This inverse relationship highlights how surface hydrophobicity increases as G_{ads} increases.

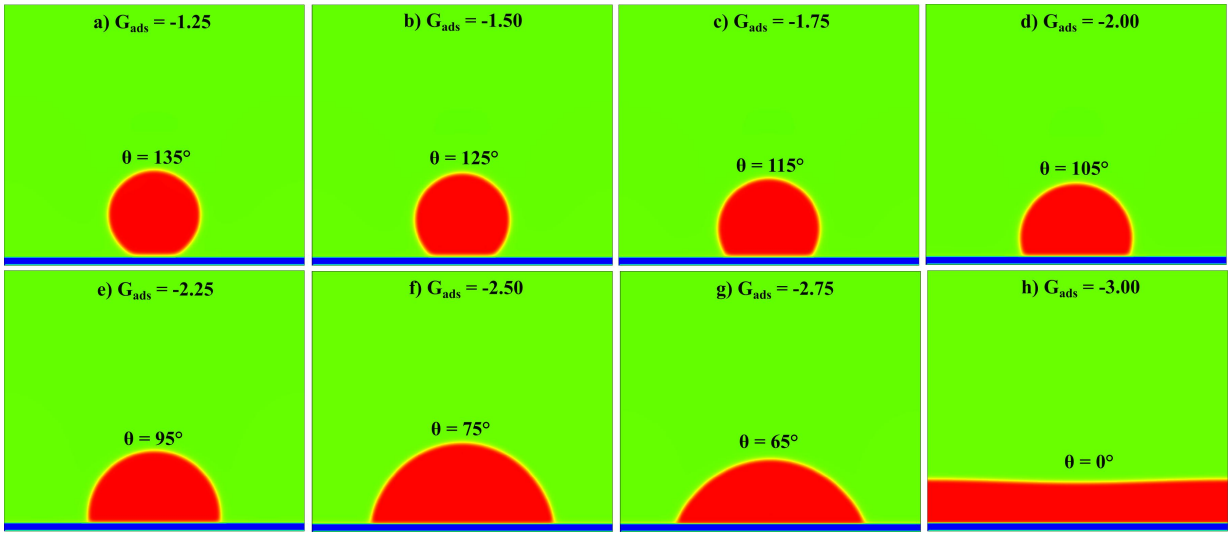

Figure 5. Effect of G_{ads} on surface wettability.

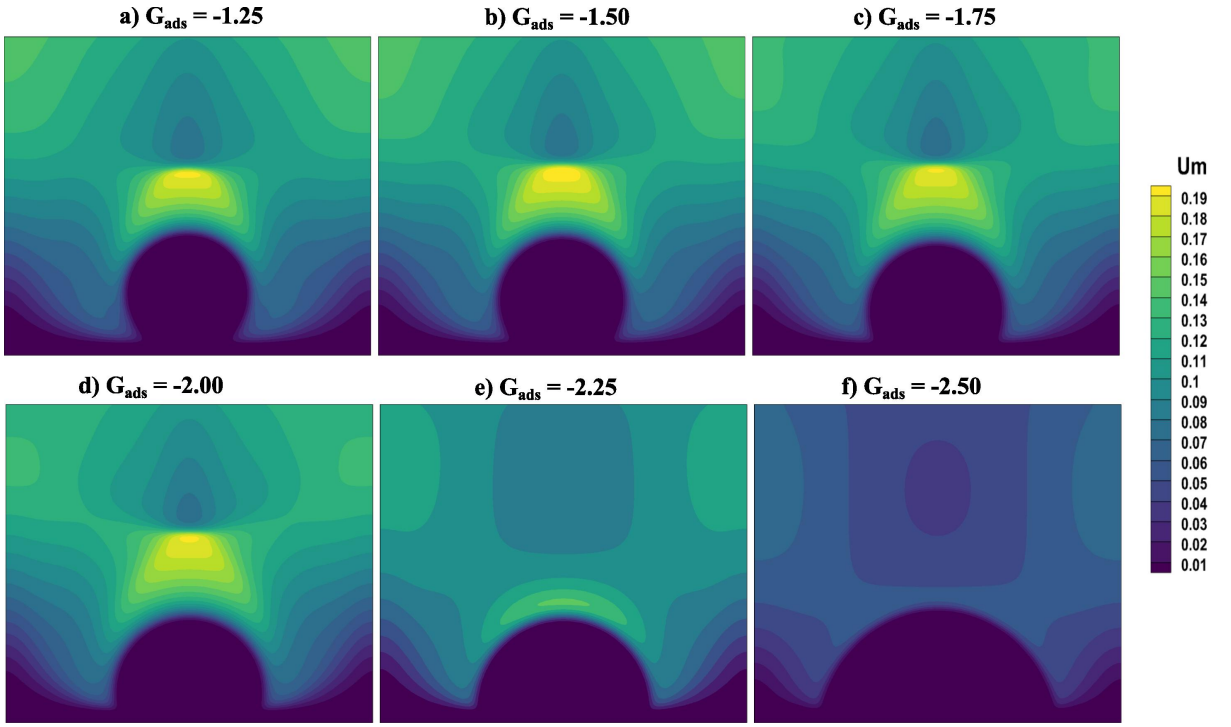

Figure 6. Effect of G_{ads} on the velocity magnitude.

3.2. Effect of G_{ads} on surface wettability

Table 1 provides a detailed examination of the effect of varying G_{ads} values on the contact angle, an important measure of surface wettability. As the solid-fluid interaction strength, represented by G_{ads}, becomes more negative, there is a noticeable reduction in the contact angle, indicating increased hydrophobicity. For instance, when G_{ads} decreases from -1.5 to -1.75, the contact angle drops from 125° to 115°, reflecting a percentage decrease of 8.00%. Similarly, as G_{ads} shifts from -1.75 to -2.0, the contact angle reduces by 8.70%, reaching 105°. This trend continues, with a 9.52% decrease when G_{ads}

Table 1. Contact angles and percentage change for varying G_{ads} values

G_{ads}	**Contact Angle (°)**	**Percentage Change in Contact Angle (%)**
-1.5	125	8.00
-1.75	115	8.70
-2.0	105	9.52
-2.25	95	10.53
-2.5	75	26.67
-2.75	65	15.38

reaches -2.25, where the contact angle becomes 95°. The most significant decrease of 26.67% is observed between $G_{ads} = -2.25$ and $G_{ads} = -2.5$, reducing the contact angle to 75°. Finally, for $G_{ads} = -2.75$, the contact angle is further reduced to 65°, showing a 15.38% decrease. These results demonstrate the inverse relationship between G_{ads} and contact angle, highlighting stronger hydrophobic behavior with increasing negative G_{ads} values.

In Figure 5, we observe the influence of the solid-fluid interaction parameter (G_{ads}) on surface wettability. The range of G_{ads} explored is from -1.25 to -3.00, and the corresponding contact angles are measured at 135°, 125°, 115°, 105°, 95°, 75°, 65°, and 0°, respectively. The interplay between cohesive forces (attraction between liquid molecules) and adhesive forces (attraction between solid and liquid) is pivotal in determining the contact angle. A higher contact angle signifies the inclination of the droplet to form a bead, indicating that either cohesive or adhesive forces dominate, with the stronger force leading to a larger contact angle.

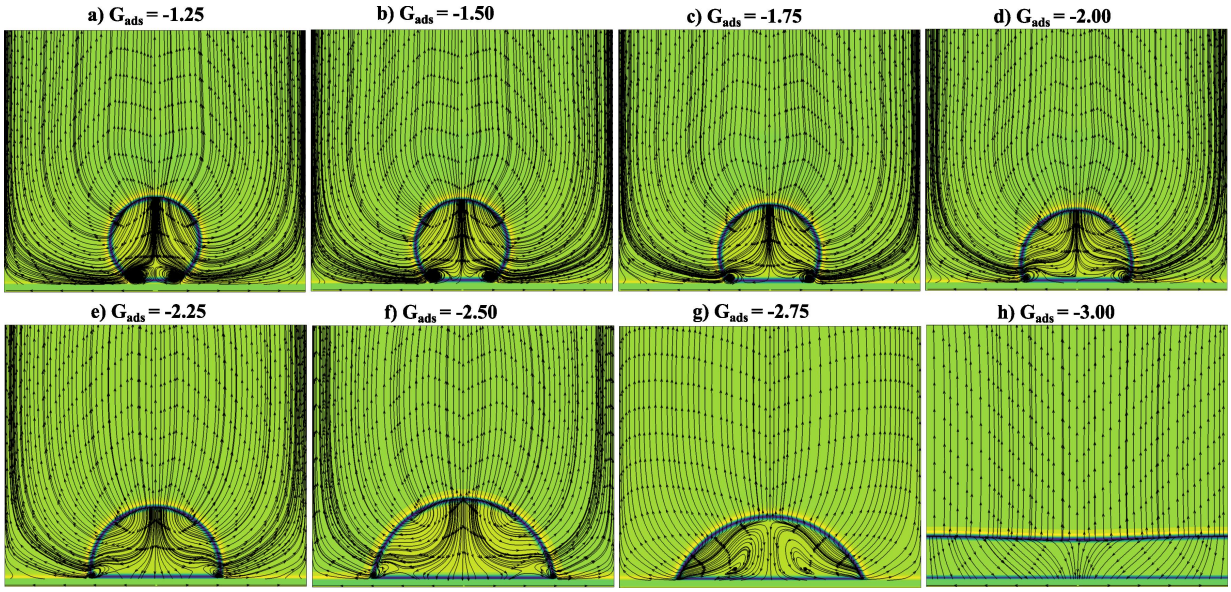

Figure 7. Effect of the G_{ads} on streamline patterns.

3.3. Effect of G_{ads} on the velocity magnitude

The contours of velocity magnitude of the water droplet with respect to vapour are shown in Figure 6 for different G_{ads} values. The inner surface of the water droplet exhibits the lowest velocity magnitude, while the maximum magnitude is seen at a distance of 0.19 [lu/ls] from it. As Figure 7 illustrates, there is a significant amount of dual circulation occurring within the water droplet. The streamline patterns show an

increase in double circulation intensity that corresponds with an increase in G_{ads}. It was observed that this phenomenon was mostly caused by the forces balancing between fluids and a solid substrate. Compared to the cohesive forces seen in vapor, the cohesive forces shown by water droplets are more noticeable.

3.4. Effect of G_{ads} on the streamline patterns

Figure 7 shows the evolution of streamline patterns generated during the droplet spreading process as a result of variations in the solid-fluid interaction parameter, denoted as G_{ads}. As G_{ads} decreases, the droplet exhibits varying degrees of wetting behavior, influencing the fluid flow surrounding it. In the upper set of images, the streamlines depict fluid motion as the droplet spreads over the surface. For higher G_{ads} values (e.g., $G_{ads} = -1.5$), the droplet exhibits limited spreading, resulting in a more compact shape with the streamlines tightly concentrated around the droplet's perimeter. As the G_{ads} value decreases to -2.0 and -2.25, the droplet experiences greater spreading, and the streamlines broaden significantly, indicating a more pronounced fluid motion away from the center of the droplet. In the lower set of images, corresponding to even lower G_{ads} values such as -2.5 and -2.75, the droplet flattens considerably, and the streamlines become more dispersed, reflecting an enhanced spreading behavior. The interactions between the droplet and the solid surface, driven by changes in G_{ads}, induce variations in fluid velocity and flow structure, leading to a significant impact on surface wetting dynamics.

4. Conclusions

In this study, we have conducted a computational exploration to examine how varying the strength of interaction between solids and fluids influences the behavior of static water droplets on smooth surfaces. We have used a two-dimensional pseudo-potential single-component multiphase lattice Boltzmann method with the $D2Q9$ model.

- The solid-fluid interaction parameter was systematically adjusted within the range of -1.25 to -3.00 to analyze its impact on wettability. As G_{ads} increases from -3.00 to -1.25, the contact angle increases from 1° to 135°, and the base diameter reduces from 200 units to 48 units, indicating enhanced hydrophobicity and reduced droplet spreading.
- As interaction strength between the solid and fluid walls, or G_{ads}, escalates, the static contact angle for textured surfaces also rises, improving the hydrophobicity of the surfaces.
- Lower G_{ads} values allow the water droplet to disperse much more quickly, which reduces internal circulation.
- The velocity magnitude is acquired more for lower G_{ads} than for higher G_{ads} because of the larger spreading rate.
- As G_{ads} decreases from -1.5 to -2.75, the droplet spreading increases significantly, leading to wider and more dispersed streamline patterns, which indicate enhanced fluid motion around the droplet.

Future Scope

The study of surface wettability using a microdroplet offers several exciting directions for future research. A primary avenue is the extension of the numerical approach to investigate the impact of complex surface textures and chemical heterogeneities on wettability characteristics. This could lead to an enhanced understanding of how various microstructures and surface coatings influence droplet behavior, thereby improving applications in microfluidics, lab-on-a-chip devices, and surface coatings.

Moreover, incorporating more advanced computational techniques, such as machine learning algorithms, can help predict surface wettability based on droplet behavior more efficiently [15]. This integration would support real-time analysis and facilitate the development of predictive models applicable to diverse materials.

Additionally, studies could focus on how wettability characteristics evolve under dynamic conditions, such as varying temperatures, fluid compositions, or under different external forces. This can be particularly relevant in fields like biomedical engineering, where surface-fluid interactions are often complex and dynamic.

Future work could also consider multi-scale modeling approaches that bridge microscopic and macroscopic interactions, offering a more comprehensive understanding of wettability across scales. Furthermore, experimental validation of numerical models through precise droplet manipulation technologies could solidify the reliability of the predictions. Lastly, applying this analysis in interdisciplinary fields like energy storage, desalination, and anti-fouling surfaces could open new applications and drive innovation across industries.

Acknowledgments

The paper was presented in the International Conference on Advances in Renewable and Green Energy Technology (ICARGET 2023). Authors also would like to acknowledge the CFD laboratory, IIT Kharagpur for providing computational facilities in support of this work.

Funding: Please add: "This research received no external funding" or "This research was funded by NAME OF FUNDER grant number XXX."

Author contributions: "Conceptualization, G. S. M and G.B.; Methodology, G.S.M., G.B.; Software, G.S.M.; Validation, G.S.M., G.B. and A.K.; Formal Analysis, G.S.M.; Investigation, G.S.M.; Resources, G.S.M.; Data Curation, G.S.M.; Writing – Original Draft Preparation, G.S.M.; Writing – Review & Editing, G.S.M., B.B., A.K; Visualization, G.S.M.; Supervision, G.B.

Disclosure statement: The authors declare no conflict of interest.

References

[1] Ganesh Sahadeo Meshram, Gloria Biswal, and Deepak Deshmukh. Effect of solid-fluid interaction parameter on wettability of surfaces with irregular triangular micropillars using lattice boltzmann method. In *2023 International Conference on Energy, Materials and Communication Engineering (ICEMCE)*, pages 1–6, 2023.

[2] Ganesh Sahadeo Meshram, Gloria Biswal, and Sasidhar Kondaraju. Numerical investigation of surface wettability with textured surfaces using lattice boltzmann method. In *2023 6th International Conference on Advances in Science and Technology (ICAST)*, pages 591–596, 2023.

[3] ABD Cassie and SJToTFS Baxter. Wettability of porous surfaces. *Transactions of the Faraday society*, 40:546–551, 1944.

[4] Panagiotis Dimitrakellis and Evangelos Gogolides. Hydrophobic and superhydrophobic surfaces fabricated using atmospheric pressure cold plasma technology: A review. *Advances in colloid and interface science*, 254:1–21, 2018.

[5] NK Adam. Use of the term 'young's equation'for contact angles. *Nature*, 180(4590):809–810, 1957.

[6] Gene Whyman, Edward Bormashenko, and Tamir Stein. The rigorous derivation of young, cassie–baxter and wenzel equations and the analysis of the contact angle hysteresis phenomenon. *Chemical Physics Letters*, 450(4-6):355–359, 2008.

[7] Robert N Wenzel. Resistance of solid surfaces to wetting by water. *Industrial & engineering chemistry*, 28(8):988–994, 1936.

[8] Li Chen, Qinjun Kang, Yutong Mu, Ya-Ling He, and Wen-Quan Tao. A critical review of the pseudopotential multiphase lattice boltzmann model: Methods and applications. *International journal of heat and mass transfer*, 76:210–236, 2014.

[9] Ganesh Meshram and Sasidhar Kondaraju. Numerical investigation of wettability and its effects on flow through textured micro-channels using lattice boltzmann method. In *Proceedings of the 26thNational and 4th International ISHMT-ASTFE Heat and Mass Transfer Conference December 17-20, 2021, IIT Madras, Chennai-600036, Tamil Nadu, India*. Begel House Inc., 2021.

[10] AA Mohamad. *Lattice boltzmann method*, volume 70. Springer, 2011.

[11] Liangliang Cao, Andrew K Jones, Vinod K Sikka, Jianzhong Wu, and Di Gao. Anti-icing superhydrophobic coatings. *Langmuir*, 25(21):12444–12448, 2009.

[12] Timm Krüger, Halim Kusumaatmaja, Alexandr Kuzmin, Orest Shardt, Goncalo Silva, and Erlend Magnus Viggen. The lattice boltzmann method. *Springer International Publishing*, 10(978-3):4–15, 2017.

[13] MC Sukop and DT Thorne. An introduction for geoscientists, 2006.

[14] Nilesh D Pawar, Sunil R Kale, Supreet Singh Bahga, Hassan Farhat, and Sasidhar Kondaraju. Study of microdroplet growth on homogeneous and patterned surfaces using lattice boltzmann modeling. *Journal of Heat Transfer*, 141(6):062406, 2019.

[15] Ganesh Sahadeo Meshram, Suman Chakraborty, and Partha P Chakrabarti. Deep learning perspectives on surface wettability: Lstm predictions for water droplet contact angles. In *2023 1st DMIHER International Conference on Artificial Intelligence in Education and Industry 4.0 (IDICAIEI)*, volume 1, pages 1–6. IEEE, 2023.